ELectronics EXpress

LETTER

IEICE Electronics Express, Vol.15, No.6, 1–6

Analysis of pulse responses from conducting strips with dispersion medium sandwiched air layer

Ryosuke Ozaki[a)] **and Tsuneki Yamasaki**[b)]

College of Science and Technology, Nihon University,

1–8–14 Surugadai, Kanda, Chiyoda-ku, Tokyo 101–8308, Japan

a) *ozaki.ryousuke@nihon-u.ac.jp*

b) *yamasaki.tsuneki@nihon-u.ac.jp*

Abstract: In this paper, we analyzed the pulse response from conducting strips with dispersion medium sandwiched air layer by using a combination of fast inversion of Laplace transform (FILT) method and point matching method (PMM), and investigated from pulse response the influence of periodically conducting strips and depth of air layer. From numerical results, we clarified the effect of the air layer, and characteristics of both air layer and periodically conducting strips are showed by differential waveform.

Keywords: pulse response, conducting strips, dispersion media, FILT, point matching method

Classification: Electromagnetic theory

References

[1] R. Persico: *Introduction to Ground Penetrating Radar—Inverse Scattering and Data Processing* (Wiley, 2013).

[2] M. Sato: "Subsurface imaging by ground penetrating radar," IEICE Trans. Electron. (Japanese Edition) **J85-C** (2002) 520.

[3] M. Nishimoto, *et al.*: "Classification of landmine-like objects buried under rough ground surfaces using a ground penetrating radar," IEICE Trans. Electron. **E90-C** (2007) 327 (DOI: 10.1093/ietele/e90-c.2.327).

[4] J. Sonoda, *et al.*: "Characteristics of detection for cavity under reinforced concrete using ground penetrating radar by FDTD method," IEICE Trans. Electron. **J100-C** (2017) 302.

[5] P. Shangguan and I. L. Al-Qadi: "Calibration of FDTD simulation of GPR signal for asphalt pavement compaction monitoring," IEEE Trans. Geosci. Remote Sens. **53** (2015) 1538 (DOI: 10.1109/TGRS.2014.2344858).

[6] R. Ozaki, *et al.*: "Numerical analysis of pulse responses in the dispersion media," IEICE Trans. Electron. **E97-C** (2014) 45 (DOI: 10.1587/transele.E97.C.45).

[7] R. Ozaki and T. Yamasaki: "Analysis of pulse reflection responses from periodic perfect conductor in two dispersion media," IEICE Trans. Electron. **E100-C** (2017) 80 (DOI: 10.1587/transele.E100.C.80).

[8] R. Ozaki and T. Yamasaki: "Pulse reflection response from two dispersion media with conducting strips," 32nd URSI GASS, **B27-2** (2017).

[9] R. Ozaki and T. Yamasaki: "Numerical analysis of pulse response from

DOI: 10.1587/elex.15.20180112
Received February 2, 2018
Accepted February 13, 2018
Publicized March 7, 2018
Copyedited March 25, 2018

periodically conducting strips with air region in dispersion media," IEICE Tech. Report, EMT2017-62 (2017) 137 (in Japanese).
[10] T. Hosono: "Numerical inversion of Laplace transform and some applications to wave optics," Radio Sci. **16** (1981) 1015 (DOI: 10.1029/RS016i006p01015).

1 Introduction

Recently, deterioration such as tunnel or the road which is constructed in high economic growth period becomes very important problem in Japan. In the subsurface of urban area, the object such as communication cables and water pipe exists in soil. Therefore, in the case of construction, we are required to examine without destroying the target objects buried in the soil. Then, the ground penetrating radar is known as technology which can investigate the geometry in underground structure [1, 2, 3, 4, 5]. However, though it is not treated the dispersion of underground medium, many numerical results are analyzed the inverse scattering problem by finite difference time domain (FDTD) method [4, 5].

In recent papers [6, 7, 8, 9], a periodic perfect conductor is used to investigate the solution for the metallic scatterer problem in soil. We have analyzed the pulse reflection responses from the periodic perfect conductor in two dispersion media by varying the parameters for the permittivity properties of the complex dielectric constants, and investigated the influence of both the dielectric and conductor using a combination of fast inversion of Laplace transform (FILT) method [10] and point matching method (PMM).

In this paper, we analyzed the pulse response from conducting strips with dispersion medium sandwiched air layer, and investigated from the pulse response the influence of periodically conducting strips and depth of air layer. Consequently, we clarified the effect of the air layer, and characteristics of both air layer and periodically conducting strips are showed by differential waveform.

2 Method of analysis

We consider the structure for periodically conducting strips with dispersion medium sandwiched air layer as shown in Fig. 1. The structure is uniform in the z-direction, and is periodic length p in the y-direction. The dielectric constant of regions S_1, S_2, S_3, and S_4 is $\varepsilon_0, \varepsilon_1, \varepsilon_2, \varepsilon_3$, respectively. The permeability is assumed to be μ_0 in all regions. A conducting strips and reflected plate is assumed to be perfectly conductor. They are embedded at $x = d_0 + d_1$ and $x \triangleq d\ (= d_0 + d_1 + d_2)$, respectively. The width of conducting strips is defined as w. In this paper, electromagnetic fields $\tilde{E}$ and $\tilde{H}$ represent those in the complex frequency domain. The waveform of the incident pulse at $x = 0$ is assumed to be a sine pulse in complex frequency domain, as in Fig. 2(a), and it can be expressed as [6, 7, 8, 9]

$$\tilde{E}_0^{(i)} = \frac{(2\pi/t_w)}{s^2 + (2\pi/t_w)^2}(1 - e^{-st_w}), \tag{1}$$

where t_w ($\triangleq 1/f_0$, f_0: center frequency) is the pulse width. The reflected wave can be expanded as the truncation mode number N_1 by using the Floquet's theorem as follows:

DOI: 10.1587/elex.15.20180112
Received February 2, 2018
Accepted February 13, 2018
Publicized March 7, 2018
Copyedited March 25, 2018

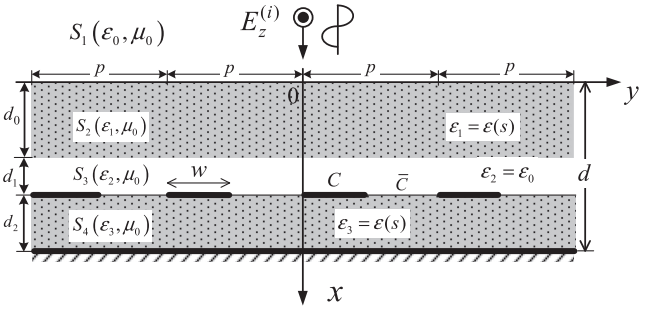

Fig. 1. Structure and coordinate system of conducting strips with dispersion medium sandwiched air layer

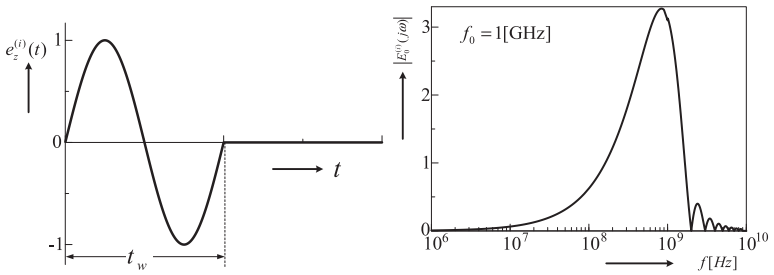

(a) waveform (b) frequency spectrum

Fig. 2. Waveform and frequency spectrum of incident sine pulse

$$\tilde{E}_z^{(r)}(x,y)=\sum_{n=-N_1}^{N_1} R_n e^{k_1^{(n)}x-i\frac{2n\pi}{p}y}. \tag{2}$$

In regions S_1, S_2, S_3, and S_4, the electromagnetic fields are expressed as [6, 7, 8, 9]

$$\tilde{E}_z^{(1)}(x,y)=\tilde{E}_0^{(i)}e^{-\tilde{k}_1 x}+\tilde{E}_z^{(r)}(x,y), \tag{3}$$

$$\tilde{E}_z^{(2)}(x,y)=\sum_{n=-N_1}^{N_1}[A_n^{(1)}e^{-k_2^{(n)}x}+B_n^{(1)}e^{+k_2^{(n)}x}]e^{-i2n\pi y/p}, \tag{4}$$

$$\tilde{E}_z^{(3)}(x,y)=\sum_{n=-N_1}^{N_1}[A_n^{(2)}e^{-k_3^{(n)}x}+B_n^{(2)}e^{+k_3^{(n)}x}]e^{-i2n\pi y/p}, \tag{5}$$

$$\tilde{E}_z^{(4)}(x,y)=\sum_{n=-N_1}^{N_1}[A_n^{(3)}e^{-k_4^{(n)}x}+B_n^{(3)}e^{+k_4^{(n)}x}]e^{-i2n\pi y/p}, \tag{6}$$

$$\tilde{H}_y^{(j)}(x,y)\triangleq\frac{1}{\mu_0 s}\frac{\partial\tilde{E}_z^{(j)}(x,y)}{\partial x},\quad (j=1\sim 4), \tag{7}$$

$$k_j^{(n)}\triangleq\sqrt{k_j^2-(-i2n\pi/p)^2},\quad k_j\triangleq s\sqrt{\varepsilon_{j-1}\mu_0}, \tag{8}$$

where k_j is wave number in the vacuum, $k_j^{(n)}$ is the propagation constant in the x-direction, and N_1 is the truncation mode number of electromagnetic fields. A_n, B_n are the unknown coefficients to be determined from boundary conditions. Here, to express the dispersion media, complex dielectric constants are employed by the combination with Sellmeier's formula and orientational polarization as follows [6]:

$$\frac{\varepsilon(s)}{\varepsilon_0}\triangleq\sum_{l=1}^{3}\frac{\Theta_l^2}{s^2+g_l s+\omega_l^2}+\frac{\kappa_l}{1+s\tau_l}. \tag{9}$$

The parameters $(\Theta_l, g_l, \omega_l, \kappa_l, \tau_l)$ of Eq. (9) were found from Ref. [6]. From the boundary condition based on Eqs. (1)–(7), we derive the simultaneous equation for

DOI: 10.1587/elex.15.20180112
Received February 2, 2018
Accepted February 13, 2018
Publicized March 7, 2018
Copyedited March 25, 2018

reflection coefficients R_n. To get this, we divided into a perfectly conducting region C and gap region $\bar{C}$ at $x = d_0 + d_1$, and apply the point matching method as following equation [7, 8, 9]:

$$Y_\alpha \triangleq \frac{y}{p} = \frac{\alpha}{2N_1 + 1}, \quad \alpha = 1 \sim (2N_1 + 1). \tag{10}$$

Therefore, boundary conditions are as follows:

$$\tilde{E}_z^{(1)}(0, y) = \tilde{E}_z^{(2)}(0, y),\ \tilde{H}_y^{(1)}(0, y) = \tilde{H}_y^{(2)}(0, y), \tag{11}$$

$$\tilde{E}_z^{(2)}(d_0, y) = \tilde{E}_z^{(3)}(d_0, y),\ \tilde{H}_y^{(2)}(d_0, y) = \tilde{H}_y^{(3)}(d_0, y), \tag{12}$$

$$Y_\alpha \in C;\ \tilde{E}_z^{(3)}(d_0 + d_1, y) = \tilde{E}_z^{(4)}(d_0 + d_1, y) = 0, \tag{13}$$

$$Y_\alpha \in \bar{C};\ \tilde{E}_z^{(3)}(d_0 + d_1, y) = \tilde{E}_z^{(4)}(d_0 + d_1, y),\ \tilde{H}_y^{(3)}(d_0 + d_1, y) = \tilde{H}_y^{(4)}(d_0 + d_1, y), \tag{14}$$

$$\tilde{E}_z^{(4)}(d, y) = 0. \tag{15}$$

From Eqs. (11)–(15), we can obtain the simultaneous equation in regard to reflection coefficients R_n,

$$Y_\alpha \in C;\ \sum_{N=-N_1}^{N_1} [\xi_1^{(n)} e^{-k_3^{(n)} d_1} + \xi_2^{(n)} e^{+k_3^{(n)} d_1}] R_n e^{-i\frac{2n\pi y}{p}} = -(\xi_3^{(0)} e^{-k_3^{(0)} d_1} + \xi_4^{(0)} e^{+k_3^{(0)} d_1}) \tilde{E}_0^{(i)}, \tag{16}$$

$$Y_\alpha \in \bar{C};\ \sum_{n=-N_1}^{N_1} [K_n^{(-)} \xi_1^{(n)} e^{-k_3^{(n)} d_1} + K_n^{(+)} \xi_2^{(n)} e^{+k_3^{(n)} d_1}] R_n e^{-i\frac{2n\pi y}{p}} = -(K_0^{(-)} \xi_3^{(0)} e^{-k_3^{(0)} d_1} + K_0^{(+)} \xi_4^{(0)} e^{+k_3^{(0)} d_1}) \tilde{E}_0^{(i)}, \tag{17}$$

where,

$\Gamma_{1,n}^{(+)} \triangleq 1 + k_1/k_2^{(n)}$, $\Gamma_{1,n}^{(-)} \triangleq 1 - k_1/k_2^{(n)}$, $\Gamma_{2,n}^{(+)} \triangleq 1 + k_1^{(n)}/k_2^{(n)}$, $\Gamma_{2,n}^{(-)} \triangleq 1 - k_1^{(n)}/k_2^{(n)}$,
$\Gamma_{3,n}^{(+)} \triangleq 1 + k_2^{(n)}/k_3^{(n)}$, $\Gamma_{3,n}^{(-)} \triangleq 1 - k_2^{(n)}/k_3^{(n)}$, $K_n^{(-)} \triangleq k_4^{(n)}\beta_n - k_3^{(n)}$, $K_n^{(+)} \triangleq k_4^{(n)}\beta_n + k_3^{(n)}$,
$\beta_n \triangleq (1 + e^{-2k_4^{(n)} d_2})/(1 - e^{-2k_4^{(n)} d_2})$, $\xi_1^{(n)} \triangleq \Gamma_{2,n}^{(-)}\Gamma_{3,n}^{(+)} e^{-k_2^{(n)} d_0} + \Gamma_{2,n}^{(+)}\Gamma_{3,n}^{(-)} e^{k_2^{(n)} d_0}$,
$\xi_2^{(n)} \triangleq \Gamma_{2,n}^{(-)}\Gamma_{3,n}^{(-)} e^{-k_2^{(n)} d_0} + \Gamma_{2,n}^{(+)}\Gamma_{3,n}^{(+)} e^{k_2^{(n)} d_0}$, $\xi_3^{(0)} \triangleq \Gamma_{1,0}^{(+)}\Gamma_{3,0}^{(+)} e^{-k_2^{(0)} d_0} + \Gamma_{1,0}^{(-)}\Gamma_{3,0}^{(-)} e^{k_2^{(0)} d_0}$,
$\xi_4^{(0)} \triangleq \Gamma_{1,0}^{(+)}\Gamma_{3,0}^{(-)} e^{-k_2^{(0)} d_0} + \Gamma_{1,0}^{(-)}\Gamma_{3,0}^{(+)} e^{k_2^{(0)} d_0}$.

The reflection coefficients is found by Eqs. (16)–(17). The reflection electric fields of Eq. (2) obtained utilizing the value of R_n is transformed into the normalized time domain using the FILT method as following equations [10]:

$$e_z^{(r)}(T) \triangleq \frac{1}{2\pi i} \int_{\gamma - i\infty}^{\gamma + i\infty} E_z^{(r)}(S) e^{ST} dS = \frac{e^a}{T} \left(\sum_{n=1}^{N-1} F_n - 2^{-(J+1)} \sum_{q=0}^{J} G_{Jq} F_{N+q} \right), \tag{18}$$

where,

$$F_n \triangleq (-1)^n \operatorname{Im}\left\{ E_z^{(r)}\left(\frac{a + i(n - 0.5)\pi}{T} \right) \right\},\ G_{JJ} \triangleq 1,\ G_{Jq-1} \triangleq G_{Jq} + \frac{(J+1)!}{q!(J+1-q)!}.$$

3 Numerical results

In the parameters of the complex dielectric constant, we use the value obtained from Ref. [6]. Here, FILT parameters of numerical calculation use $a = 4$, $J = 10$, and $N = 50$. In the following analysis, we assumed to be dielectric constant $\varepsilon_2 = \varepsilon_0$.

Fig. 3(a) shows the result of pulse responses for varying normalized depth of air layer D_1 ($\triangleq d_1/p$) as condition of a normalized depth D_2 ($\triangleq d_2/p$) = 100,

DOI: 10.1587/elex.15.20180112
Received February 2, 2018
Accepted February 13, 2018
Publicized March 7, 2018
Copyedited March 25, 2018

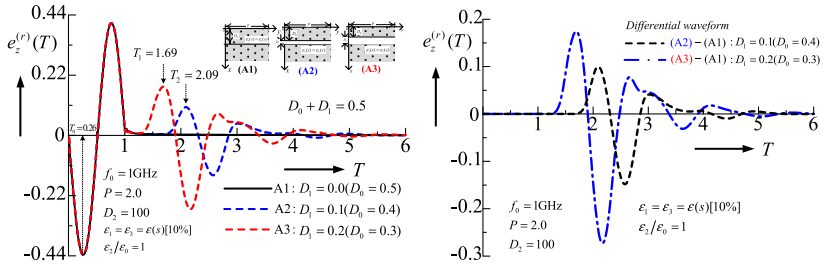

(a) Pulse response (b) Differential waveform

Fig. 3. Pulse response for varying normalized depth D_1 of air layer

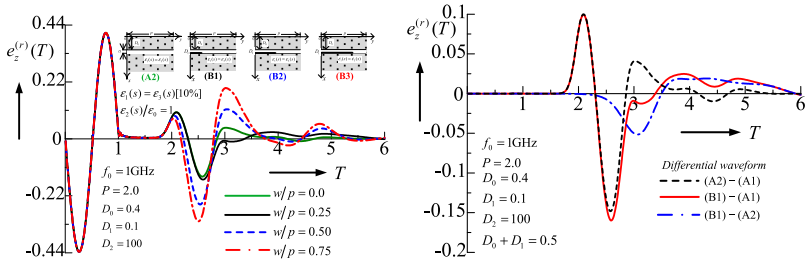

(a) Pulse response (b) Differential waveform

Fig. 4. Pulse response for varying the normalized conducting width w/p

normalized period P ($\triangleq p/(t_w c)$) $= 2.0$, $f_0 = 1$ GHz, normalized conducting width $w/p = 0.0$, and dispersion medium $\varepsilon_1 = \varepsilon_3 = \varepsilon(s)$ of water ratio 10% for fixed normalized depth $D_0 + D_1$ ($\triangleq (d_0 + d_1)/p$) $= 0.5$. Fig. 3(b) shows the differential waveform for result of Fig. 3(a). And, we named as A1∼A3 the analysis structure in Fig. 3. From Figs. 3(a) and (b), we can see the following features:

(1) By changing the normalized depth of air layer D_1, the initial pulse response at $0 < T \leq 1$ is same for all cases. And also, we can see that time difference occurs for the response because of a propagation distance of the dispersion medium.

(2) From Fig. 3(a), we investigate the normalized thickness D_0 of the medium from the difference of peak value because of a rise time is unclear. Here, the normalized time of peak value is $T_0 = 0.26$ for case of $D_1 = 0.0$, $T_1 = 1.69$ for case of $D_1 = 0.1$, and $T_2 = 2.09$ for case of $D_1 = 0.2$, respectively. Consequently, each time difference is T_{d1} ($\triangleq T_2 - T_0$) $= 1.83$ and T_{d2} ($\triangleq T_1 - T_0$) $= 1.43$ for case of $D_0 = 0.4$ ($D_1 = 0.1$) and $D_0 = 0.3$ ($D_1 = 0.2$), respectively. On the other hand, by using the 0-th mode propagation constant $k_2^{(0)}$ and real part of complex dielectric constant $\varepsilon(s) \approx 5.8742$ at $f_0 = 1$ GHz in Ref. [6], each propagation distance is $l_{d1} = 2D_0\sqrt{\varepsilon(s)} = 0.8\sqrt{5.8742} \approx 1.94$, $l_{d2} = 2D_0\sqrt{\varepsilon(s)} = 0.6\sqrt{5.8742} \approx 1.45$. Therefore, both results are approximately same as $T_{d1} \cong l_{d1}$, $T_{d2} \cong l_{d2}$.

(3) We can see that the initial pulse response vanishes from Fig. 3(b) because of same amplitude responses. As the result, we can understand as the amplitude of response depends on the influence of the depth for the air layer.

Next, we investigate the influence of w/p. Fig. 4(a) shows the results of pulse response for varying w/p as condition of $D_0 = 0.4$ and $D_1 = 0.1$ for fixed the same condition of Fig. 3. In the same manner, we named as B1∼B3 the analysis structure in Fig. 4. For comparison of Fig. 4(a), we also showed the result of structure A2 in Fig. 3(a). Fig. 4(b) shows the differential waveform for result of Fig. 4(a). From Figs. 4(a) and (b), we can see the following features:

DOI: 10.1587/elex.15.20180112
Received February 2, 2018
Accepted February 13, 2018
Publicized March 7, 2018
Copyedited March 25, 2018

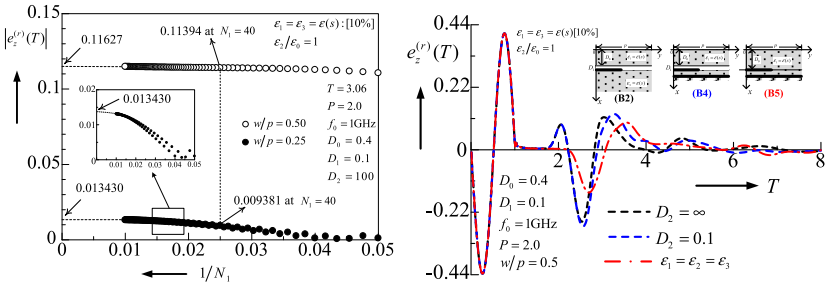

(a) Convergence of $1/N_1$ (b) Comparison of pulse response

Fig. 5. Convergence of $1/N_1$ and comparison of pulse response

(1) By changing the w/p, we can see that the pulse amplitude from air layer for $w/p = 0.0$ at $2.2 \leq T \leq 2.79$ is smallest in all the cases. But, at $2.8 \leq T \leq 3.4$, its amplitude for case of $w/p = 0.25$ is smaller than that of $w/p = 0.0$.
(2) From Fig. 4(b), we can see that the effect of a conductor and air layer appear at the near $T \approx 3.0$. And, from the result of B1–A2, we can obtain only the response from strip conductor. Consequently, the phase of response for B1–A2 is opposite to that of A2–A1 for the response which is extracted the influence only from air layer.

We examine the convergence of the truncation mode number N_1 of electromagnetic fields. Fig. 5(a) shows convergence of the truncation mode number $1/N_1$ versus the normalized electric fields $|e_z^{(r)}(T)|$ for case of $w/p = 0.25$ and $w/p = 0.50$ for fixed $T = 3.06$ under the same conditions as Fig. 4. From Fig. 5(a), the relative error in the $|e_z^{(r)}(T)|$ to extrapolated true value is less than about 2% when we computed by using $N_1 \geq 40$. However, in the case of $w/p = 0.25$, we can see that it is not sufficient to use for this calculation. Therefore, we can understand that it have to use $N_1 \geq 90$ in order to maintain the same accuracy as $w/p = 0.50$. Finally, we investigate the influence of reflected plate under the same conditions as Fig. 4.

Fig. 5(b) shows the pulse responses for both $w/p = 0.50$, $D_1 = 0.1$ and $w/p = 0.50$, $D_1 = 0.0$ under the same condition of Fig. 4. For comparison, we also show the result for $D_2 = \infty$ ($\cong 100$) from Fig. 4(a). From Fig. 5(b), we can see the following features:
(1) From the results of $D_2 = \infty$ and $D_1 = 0.1$, we can see the slightly effect of the reflected plate from near $T = 2.5$. Thus, we can consider that it appears only influence of the conductor because of the depth D_2 of dispersion medium is thin layer.
(2) In comparison with case of same media $\varepsilon_1 = \varepsilon_2 = \varepsilon_3$, we can see the amplitude of response becomes smaller than that of other case. As this reason, we can be considered as the response attenuated by the effect of dispersion medium.

4 Conclusions

In this paper, we analyzed the pulse response from conducting strips with dispersion medium sandwiched air layer, and investigated the influence of periodically conducting strips, air layer, and the reflected plate by using a combination of FILT and PMM methods.

From numerical analysis, we clarified the effect of the air layer, periodically conducting strips, the reflected plate by using the differential waveform. As a result, we were able to obtain the characteristics for the layer of target objects.

DOI: 10.1587/elex.15.20180112
Received February 2, 2018
Accepted February 13, 2018
Publicized March 7, 2018
Copyedited March 25, 2018